# Blood DNA methylation analysis reveals a distinctive epigenetic signature of vasospasm in aneurysmal subarachnoid hemorrhage

Isabel Fernández-Pérez, MD[1,2], Joan Jiménez-Balado, PhD[2], Adrià Macias-Gómez, MD[1,2], Antoni Suárez-Pérez, MD[1,2], Marta Vallverdú-Prats, PhD[2], Alberto Perez Giraldo, MD[3], Marc Viles, MD[4], Julia Peris, MD[1], Sergio Vidal, MD[1], Eva Giralt-Steinhauer, MD, PhD[1,2,5], Daniel Guisado-Alonso MD, PhD[1,2], Manel Esteller, MD, PhD[6,7], Ana Rodriguez-Campello, MD, PhD[1,2,5], Jordi Jiménez-Conde, MD, PhD[1,2,5], Angel Ois, MD, PhD*[1,2,5], Elisa Cuadrado-Godia, MD, PhD*[1,2,5]

1. Neurology Department, Hospital del Mar, Barcelona, Catalunya, Spain
2. Neurovascular Research Group, Hospital del Mar Medical Research Institute, Barcelona, Catalunya, Spain
3. Neurosurgery Department, Hospital del Mar, Barcelona, Catalunya, Spain
4. Neuroradiology Department, Hospital del Mar, Barcelona, Catalunya, Spain
5. Pompeu Fabra University, Barcelona, Catalunya, Spain
6. Cancer Epigenetics Group, Research Institute Against Leukemia Josep Carreras, Badalona, Catalunya, Spain
7. Physiological Sciences Department, School of Medicine and Health Sciences, University of Barcelona, Barcelona, Catalunya, Spain

**contributed as last authors.*

Corresponding author: Joan Jiménez Balado. Neurovascular Research Group, Hospital del Mar Research Institute. C/Dr. Aiguader, 88, 08003, Barcelona, Spain. E-mail address: jjimenez3@researchmar.net.

Keywords: subarachnoid hemorrage, epigenetics, DNA methylation, vasospasm.

**Statements and declarations:** Authors have no potential conficts of interest to report.

**Funding:** This work was supported in part by Spain's Ministry of Health (Instituto de Salud Carlos III, Fondos FEDER, RICORS-ICTUS (RD21/0006/0021), P19/00011 and PI23/00351). Sara Borrell and Rio Hortega programs, funded by Instituto de Salud Carlos III (CD22/00001, J.J.B. and CM22/00009 A.S.P)

**Acknowledgements:** We would like to thank all the patients who agreed to participate in our study, as well as all the colleagues in the team who are involved in collecting data for the Basicmar registry.

**Author Contributions:** ECG, JJC, AO, ARC and EGS contributed to the conception and design of the study. MVP, JJB, IFP, AMG, ASP, JP, SV, MV, APG, DGA and ME contributed to the acquisition and analysis of data. IFP, ECG, JJB, AO and MVP drafted a significant portion of the manuscript and figures. All authors interpreted the data, reviewed the manuscript and approved the final version.

ABSTRACT

**Introduction:**

Vasospasm is a potentially preventable cause of poor prognosis in patients with aneurysmal subarachnoid hemorrhage (aSAH). Epigenetics might provide insight on its molecular mechanisms. We aimed to analyze the association between differential DNA methylation (DNAm) and development of vasospasm.

**Methods**

We conducted an epigenome-wide association study in 282 patients with aSAH admitted to our hospital. DNAm was assessed with the EPIC Illumina chip (>850K CpG sites) in whole-blood samples collected at hospital admission. We identified differentially methylated positions (DMPs) at the CpG level using Cox regression models adjusted for potential confounders, and then we used the DMP results to find differentially methylated regions (DMRs) and enriched biological pathways.

**Result**

A total of 145 patients (51%) experienced vasospasm. In the DMP analysis, we identified 30 CpGs associated with vasospasm at p-value < 10-5. One of them (cg26189827) was significant at the genome-wide level (p-value < 10-8), being hypermethylated in patients with vasospasm and annotated to SUGCT gene, mainly expressed in arteries. Region analysis revealed 30 DMRs, some of them annotated to interesting genes such as POU5F1, HLA-DPA1, RUFY1, and CYP1A1. Functional enrichment analysis showed involvement of biological processes related to immunity, inflammatory response, oxidative stress, endothelial nitric oxide, and apoptosis.

**Conclusion**

Our findings show, for the first time, a distinctive epigenetic signature of vasospasm in aSAH, establishing novel links with essential biological pathways, including inflammation, immune responses, and oxidative stress. Although further validation is required, our results provide a foundation for future research into the complex pathophysiology of vasospasm.

## INTRODUCTION

Aneurysmal subarachnoid hemorrhage (aSAH) is a distinct subtype of stroke, primarily affecting young women, and is marked by a significant risk of mortality and long-term disability. One of the most frequent complications is vasospasm, which can affect up to 70% of patients with aSAH[1,2]. Patients with vasospasm are at a 3-fold increased risk of poor functional and cognitive outcomes, and nearly two-fold increased risk of death[3]. Despite the high prevalence and serious consequences, effective treatments remain elusive. Therefore, understanding the mechanisms underlying vasospasm development is crucial for identifying potential therapeutic targets.

Epigenetics is the study of the mechanisms that regulate the gene expression without altering the DNA sequence. The main epigenetic mechanism is DNA methylation (DNAm), which is heritable but can be modified according to lifestyle or environmental factors[4]. Extensive research proved that DNAm participates in the pathogenesis of closely related other cerebrovascular diseases, such as ischemic stroke or intracerebral hemorrhage[5,6].

Current literature on the impact of DNAm on vasospasm remains limited, primarily focusing on genetic studies using candidate-gene approaches[7]. Specifically, two prior studies examined methylation trajectories in cerebrospinal fluid (CSF) at genes associated with iron homeostasis relation to vasospasm, yielding non-significant findings[8,9]. However, vasospasm is a complex phenomenon influenced by numerous biological mechanisms beyond iron homeostasis, such as nitric oxide, haptoglobin, inflammation or prothrombotic pathways[10,11]. Consequently, conducting epigenome-wide association studies (EWAS) utilizing microarray technologies may offer deeper insights into this phenomenon, as do not rely on previous hypothesis or assumptions[12]. Therefore, our study aimed to investigate the role of DNAm in the development of vasospasm, within a cohort of aSAH patients with comprehensive data.

## METHODS

### Study design.

We designed a prospective observational study in patients with aSAH. We first measured DNAm, and then identified differentially methylated positions (DMPs) at the CpG level using Cox regression models adjusted for potential confounders. We subsequently used the DMP results to find differentially methylated regions (DMRs) and enriched biological pathways.

### Ethics approval and consent to participate.

Cases were not formally involved in the study design or the outcome measures. The study protocol was approved by the Ethical Review Board of Parc de Salut Mar (2019/8592/I), Barcelona, Spain. This

study was conducted in accordance with the principles of the Declaration of Helsinki. All patients or their relatives signed an informed consent form to be included in the study.

**Study population.**

The study is based on a prospective registry of SAH patients (SAH-Mar)[13,14] recruited at the Hospital del Mar (Barcelona), a tertiary stroke center included in the Catalan SAH care system, that serves a population of 300.000 individuals and one weekend each month, it serves as the only referral center for all patients with a diagnosis of SAH in Catalonia (7,400,000 inhabitants). Inclusion criteria for this study were: aSAH patients, and availability of DNAm data. study. Exclusion criteria were: (1) patients transferred to other centers during the acute phase of the SAH; (2) death within the first 72h; and (3) lack of data about vasospasm. All patients were assessed and classified by a vascular neurologist. Among 423 subjects with aSAH enrolled from January 2007 to May 2020, blood samples were obtained from 411, being 64 of them additionally excluded due to fatal SAH or lack of clinical data. Among the remaining 347 eligible patients, we measured DNAm on the first 288 due to economic budget limitations, who were included in this study.

**Clinical management and Variables of the study**

The clinical management protocols and variables employed in this study adhere to established national and international guidelines, as evidenced by our previously published works[13,14].
A baseline evaluation, encompassing CT perfusion coupled with CT angiography (CTA), was conducted 24 hours following aneurysm occlusion treatment. To monitor the occurrence of vasospasm, each patient underwent daily transcranial Doppler (TCD) assessments during the initial 10 days, followed by subsequent evaluations at 48-hour intervals, thereafter, extending up to 15 days or beyond, as deemed appropriate by the attending physician. All patients were administered nimodipine at recommended doses[15,16]. In the event of a new neurological deficit attributed to vasospasm or deterioration of vasospasm despite the prescribed therapeutic regimen, a subsequent CTA and perfusion scan was performed to confirm the diagnosis, followed by the implementation of endovascular intra-arterial nimodipine and/or mechanical angioplasty. Demographics, clinical and radiological data were registered in a structured questionnaire by the neurovascular team and reviewed by the study investigators. Vasospasm was defined by specific diagnostic criteria, including a mean flow velocity exceeding 120 cm/sec in the middle cerebral artery as determined by TCD examination[16], or the observation of moderate-to-severe arterial narrowing during digital subtraction angiography or CTA, excluding factors such as atherosclerosis, catheter-induced spasm, or vessel hypoplasia. The ultimate diagnosis of vasospasm was made by a certified neuroradiologist. Additionally, we meticulously documented the date of vasospasm diagnosis and the subsequent treatment administered.

**DNA Methylation array**

DNA samples were extracted from blood, collected in 10mL EDTA tubes at the time of admission and immediately stored at -20ºC until the moment of DNA isolation. The DNA extraction was carried out using FlexiGene DNA kit (Qiagen, Germany), according to the manufacturer's protocol and stored at -20ºC. Genome-wide DNAm data was obtained in a single study batch composed of three technical runs. Bisulfite conversion of genomic DNA (1 µg) was done with the EZ-96 DNA Methylation Kit (Zymo Research, Orange, CA, USA). All samples (N=288) were analyzed using the Illumina Methylation EPIC Beadchip (Illumina, Eindhoven, Netherlands), which assesses the methylation in 865,918 CpG positions. The arrays corresponding to these samples were scanned with the Illumina HiScan SQ scannerat Progenika Biopharma in Prior to analyze the intensity data files, we started a series of quality controls (QCs) in GenomeStudio to exclude those samples that presented deviated values in the control probes, which assess the quality of different sample preparation steps (staining, extension, hybridization, target removal, bisulfite conversion, among others). Data was then processed considering several relevant quality controls[17] . In brief, intensity data files were parsed using the R-library *Minfi*[18]. Regarding sample QCs, we excluded those samples presenting sex mismatch, having a call rate lower than 98% or that represented outlier observations[17,18]. For CpG QCs, we filtered those CpG probes that had a detection *p*-value higher than 0.05 in at least 1% of samples, that had a total intensity count lower than 3 in at least 5% of samples or that showed cross-reactivity[19] . Besides, we additionally removed non- CpG probes and those located at allosomal or SNP positions[20]. After applying these QCs, 742,472 CpGs were evaluated in 285 samples (see the supplementary table 1 for additional information on these QCs). This set of CpGs were subsequently normalized to β values (ratio between methylated signal and total signal plus a constant) and normalized using a beta-mixture quantile normalization (BMIQ) method[21]. We continued exploring the density function of samples' CpGs to ensure a correct beta distribution after BMIQ normalization. We then applied a singular value decomposition of the full DNAm dataset to detect potential batch effects by exploring the first two dimensions. Thereby, we observed a batch effect related to the technical run which was subsequently removed with the *sva* library[22] (supplementary figure 1). Finally, we estimated the white blood cell counts from whole blood DNAm using the Houseman algorithm and regressed out their effect[23]. We used both the Illumina Manifest and Genomic Regions Enrichment of Annotations Tool (GREAT) software to annotate CpG to their target genes[24].

## Statistical Analyses & Bioinformatics

### 1. Descriptive analyses

Data was expressed as mean (±standard deviation), median (interquartile range) or count (percentage) according to the type and distribution of each variable. Main demographic, clinical and outcome variables were compared between patients with and without vasospasm using *t*-, U Mann-Whitney or $\chi^2$ tests, as appropriate.

### 2. Differentially methylated positions analysis

We firstly explored whether patients with and without vasospasm presented DMPs. To that aim, we first build Cox regression models in which incidence of vasospasm was the dependent variable and each CpG was entered as the predictor of interest. Follow-up time and events were right-censored at 90 days after symptoms onset according to our protocol for follow-up. These models were additionally adjusted for: age, sex, smoking habit, ethnicity and Fisher scale grade. These covariables were selected based on previous literature describing risk factors for vasospasm[25,26] and factors known to affect DNAm[27–30]. Besides, we did not include both Fisher and H&H scales to avoid potential collinearity. We checked the Cox model assumptions of a baseline model only including this set of covariables, calculating the Schoenfeld and Deviance residuals to detect outliers and confirm proportional hazard assumptions. Additionally, the effect of nominally significant candidates (*p*-value$<10^{-5}$) on vasospasm incidence was visually explored by discretizing methylation into tertiles and exploring the univariate Kaplan-Meier for each CpG. All candidates were annotated using the Illumina manifest data and the GREAT software[24]. Moreover, DMPs results were corrected by three sources of bias: 1) multiple testing; 2) presence of outliers in methylation distribution of CpG candidates; 3) test-statistic inflation. Regarding multiple testing, we applied the false discovery rate (FDR) adjustment (Benjamini-Hochberg method). To test the robustness of our results against outliers, we ran a bootstrap analysis in significant candidates at nominal *p*-value ($10^{-5}$). Briefly, we iteratively tested the effect of each CpG in 10,000 resampled sets of the original sample. This produced an empirical distribution of β coefficients, which allowed the calculation of the 0.1 and 99.9 percentiles to check whether these candidates were significant after bootstrapping our results ($\alpha$=.05/n, where 'n' represents the number of candidates). Finally, as test-statistic inflation is a common source of bias in EWAS analyses, we used the library Bacon on raw z-statistics, adjusting the inflation via a Bayesian method[31]. Given the time-dependent nature of vasospasm, a sensitivity analysis was undertaken to elucidate whether different methylation patterns observed between vasospasm-affected and unaffected patients were influenced by the temporal interval since the symptom onset. To that aim, we repeated the DMP analysis of CpG candidates at a nominal cutoff in the subgroup of participants with bleeding onset within 48h of admission. Finally, to gain insight on the role of CpG candidates (*p*-value < $10^{-5}$) on vasospasm development we checked the association of

DMP with main risk factors such as age, sex, Fisher and Hunt & Hess scales, smoking, history of hypertension and time since bleeding onset. Results were corrected by multiple testing (Bonferroni adjustment).

### 3. Differentially methylated regions analysis

We next aimed to discover DMRs among patients with vasospasm, defined as groups of CpG with specific DNAm patterns. For this purpose, we used the *comb-p* library[32]. Briefly, this library combines single CpGs *p*-values from adjacent genetic regions after accounting for their correlation and defining a window size (500kb in our case). We set the seed *p*-value to $10^{-3}$, which means that it needs at least one *p*-value $\leq 10^{-3}$ to extend the region to the next CpG within 500kb in our case. These values for seed *p*-value and window size parameters have been previously used in the literature for finding DMRs[33,34]. We only considered a region as significant when it had at least 4 CpGs and a Q-value < .05 (Sidak correction). DMRs were visually explored, by plotting the individual *p*-values of each CpG in the region against genomic coordinates. DMRs were annotated using the GREAT software[24,35,36]. Besides, we averaged the methylation levels of all CpGs conforming each region to explore whether DMRs were hyper or hypomethylated in patients with vasospasm. Finally, we explored how this average methylation at the region level was associated with main risk factors associated with vasospasm (age, sex, Fisher and Hunt & Hess scales, smoking, history of hypertension and time since aSAH onset) as we did before for DMPs.

### 4. Pathway analysis

For biological pathways analysis, we used the methylGSA R package. This library takes as input single CpG *p*-values and conducts a ranked gene set enrichment analysis (GSEA). As one gene might receive annotations from more than one CpG, their significance is averaged using the Robust Rank Aggregation method[37]. This method tests the null hypothesis that a vector of *p*-values follows a uniform distribution [0,1] after converting observed *p*-values to order statistics. Then, three different databases are tested for enrichment: Gene-Ontologies (GO), Kyoto Encyclopedia of Genes and Genomes (KEGG) and Reactome. Besides, there is the possibility to consider only CpGs from promoter regions or located at the gene-body, but, in our case, we considered all CpGs, independently of their relationship with the gene. We considered as significant those gene sets having a Q-value (FDR) lower than 0.05. We subsequently queried the list of genes annotated to significant biological pathways and calculated the similarity between two gene-sets ‘a’ and ‘b’ as:

$$Similarity_{a-b} = \frac{N \cap Genes}{N \cup Genes}$$

That is, the number of intersected genes adjusted by the union of genes, which ranges between 0 to 1 and can be interpreted as the percentage of genes in common between two pathways. We then plotted the similarity between two gene-sets as an acyclic graph where nodes were gene-sets and edges were

weighted by the similarity index. We only kept those edges having a similarity higher or equal than 0.2. Finally, we detected clusters of similar biological pathways by using the autoannotate function included in Cytoscape software.

## RESULTS

Of the initial 285 samples that met the technical QC, three were excluded due to incomplete clinical data. Consequently, our final cohort comprised 282 individuals with aSAH. Demographical and clinical data of the study population are summarized in table 1. The average age was 55.9 (±13.9) years with 187 (67%) being female. Most of the participants were identified as Caucasians (241 individuals, 85.5%). Regarding aSAH risk factors, 133 (47.2%) had history of hypertension and 106 (37.6%) were active smokers. Most patients arrived at the hospital on the same day after symptoms onset (150, 53%) and most frequent score in the Fisher and Hunt & Hess scales were 4 (184 individuals, 65.2%) and 2 (152 individuals, 53.9%), respectively. A total of 145 patients (51.4%) developed vasospasm. In the univariate analyses, age and days from symptom onset to hospital arrival were associated with vasospasm (table 1). Specifically, younger patients, who arrived at the hospital later, exhibited a higher probability of experiencing vasospasm. Concerning DCI, it occurred in 71 individuals (25.2%), 56 of them (79%) having vasospasm, and 58 of them (82%) developing an ischemic lesion.

**Table 1.** Characteristics of the cohort

| | **All (N=282)** | **Vasospasm (N=145)** | **No vasospasm (N=137)** | ***p*-value** |
|---|---|---|---|---|
| Age | 55.9 [±13.9] | 53.4[±12.4] | 58.5 [±15.0] | 0.002 |
| Female gender | 189 (67.0%) | 105 (72.4%) | 84 (61.3%) | 0.064 |
| Ethnicity: | | | | 0.888 |
| Caucasian | 241 (85.5%) | 123 (84.8%) | 118 (86.1%) | |
| Other | 41 (14.5%) | 22 (15.2%) | 19 (13.9%) | |
| Hypertension | 133 (47.2%) | 61 (42.1%) | 72 (52.6%) | 0.100 |
| Smoker | 106 (37.6%) | 61 (42.1%) | 45 (32.8%) | 0.140 |
| Fisher: | | | | 0.735 |
| 1 | 9 (3.19%) | 3 (2.07%) | 6 (4.38%) | |
| 2 | 23 (8.16%) | 12 (8.28%) | 11 (8.03%) | |
| 3 | 66 (23.4%) | 33 (22.8%) | 33 (24.1%) | |
| 4 | 184 (65.2%) | 97 (66.9%) | 87 (63.5%) | |
| Hunt & Hess: | | | | 0.821 |
| 1 | 6 (2.13%) | 2 (1.38%) | 4 (2.92%) | |
| 2 | 152 (53.9%) | 82 (56.6%) | 70 (51.1%) | |
| 3 | 59 (20.9%) | 29 (20%) | 30 (21.9%) | |
| 4 | 32 (11.3%) | 15 (10.3%) | 17 (12.4%) | |
| 5 | 33 (11.7%) | 17 (11.7%) | 16 (11.7%) | |
| Days until arrival (days) | 0 [0-3] | 1 [0-4] | 0 [0-2] | 0.016 |
| DCI | 71 (25.2%) | 56 (38.6%) | 15 (10.9%) | <0.001 |
| IS due to DCI | 58 (20.6%) | 44 (30.3%) | 14 (10.2%) | <0.001 |
| Vasospasm | 145 (51.4%) | - | - | - |
| Vasospasm onset (day) | 4 [2-7] | - | - | - |

**Table 1. Characteristics of the cohort**. Summarized data in the whole sample and by vasospasm groups (presence or absence). Univariate contrasts have been performed using *t*-, U-Mann Whitney or $X^2$ tests, as appropriate. DCI: Delayed cerebral ischemia. IS: ischemic stroke

## Differentially methylated positions analysis

We identified 31 CpGs that were associated with vasospasm at *p*-value < $10^{-5}$ (figure 1a and table 2), being most of them hypermethylated (77.4%). One CpG (cg26189827) was significant at the genome-wide level (*p*-value < $10^{-8}$), being hypermethylated in patients with vasospasm and annotated to Succinyl-CoA: Glutarate-CoA Transferase (*SUGCT*) gene. The CpG cg26189827 showed a Hazard ratio of 1.13, which indicates that for each 1% increase in methylation in this CpG, we observed a 13% increased risk of vasospasm within the follow-up. To visualize the effect of methylation at these CpG positions on the risk of vasospasm, we discretized methylation for each CpG according to quartiles distribution, and then we plotted the Kapplan-Meier curves (figure 1b and supplementary figure 2). Interestingly, we observed an upward trend among the majority of CpG candidates indicating that individuals with increased methylation at these sites were more prone to an earlier onset of vasospasm.

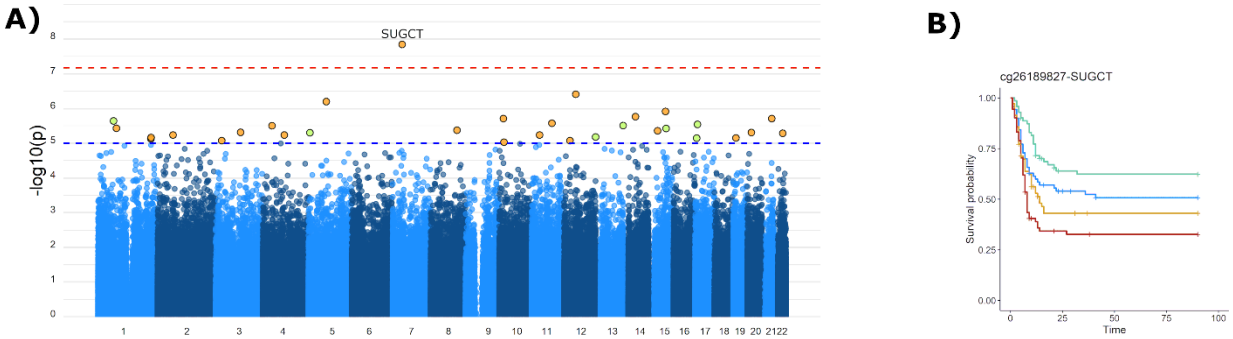


**Figure 1** Genome-wide association DNA methylation study of vasospasm. Panel A: Manhattan plot. Each dot represents a CpG annotated according to the Hg38 genomic coordinates (X) and -log10 p-value (Y axis). Green and orange dots are those CpG with a p-value <1x10-5, with green color indicating hypomethylation in individuals with vasospasm, and orange color indicating hypermethylation. The blue and red dashed line represent the cutoffs for nominal and genome-wide significant, respectively. Panel B: Kapplan-Meier curve representing the effect of cg26189827 (SUGCT, p-value=1.43·10-8) on the incidence of vasospasm. The X axis represents time since symptoms onset in days, while the Y axis represents the survival function. Groups have been obtained by discretizing methylation (β values) for the CpG according to quartiles distribution (light blue: first quartile; blue: second quartile; yellow: third quartile; red: fourth quartile)

*Keywords: SUGCT: Succinyl-CoA:Glutarate-CoA Transferase gene*

**Table 2. Differentially Methylated Positions in patients with Vasospasm**

| Annotations | | | | | | | DMP Results | | | | Sensitivity Analysis | | |
|---|---|---|---|---|---|---|---|---|---|---|---|---|---|
| **CpG** | **CHR** | **BP** | **Gene Illumina** | **Feature** | **Island** | **GREAT** | **β** | **HR** | ***p*-value** | ***p*-value Bacon** | **β** | ***p*-value** | **Bonferroni** |
| cg26189827 | 7 | 40338925 | SUGCT | Body | | SUGCT | 0.122 | 1.130 | 1.43E-08 | 1.88E-08 | 0.120 | 1.71E-05 | 5.30E-04 |
| cg16797275 | 12 | 50097773 | FMNL3 | Body | N_Shelf | FMNL3 | 0.098 | 1.102 | 3.89E-07 | 5.30E-07 | 0.098 | 5.16E-05 | 1.60E-03 |
| cg05673882 | 5 | 74862702 | POLK | Body | | ANKDD1B | 0.084 | 1.088 | 6.39E-07 | 8.72E-07 | 0.083 | 6.91E-05 | 2.14E-03 |
| cg20189274 | 15 | 69339228 | NOX5 | Body | | NOX5 | 0.147 | 1.158 | 1.22E-06 | 1.67E-06 | 0.154 | 1.95E-05 | 6.04E-04 |
| cg03745715 | 14 | 50983180 | MAP4K5 | Body | | MAP4K5 | 0.318 | 1.375 | 1.72E-06 | 2.36E-06 | 0.402 | 3.21E-06 | 9.95E-05 |
| cg13409442 | 10 | 17726728 | STAM | Body | | STAM | 0.043 | 1.044 | 1.95E-06 | 2.69E-06 | 0.039 | 3.47E-04 | 1.07E-02 |
| cg17364089 | 21 | 40139776 | LINC00114 | Body | | ETS2 | 0.061 | 1.062 | 1.96E-06 | 2.70E-06 | 0.066 | 4.51E-05 | 1.40E-03 |
| cg16904854 | 1 | 65809524 | DNAJC6 | 5'UTR | | DNAJC6 | -0.383 | 0.682 | 2.29E-06 | 6.59E-07 | -0.463 | 4.10E-06 | 1.27E-04 |
| cg04373607 | 11 | 85151996 | DLG2 | Body | | DLG2 | 0.153 | 1.165 | 2.66E-06 | 3.66E-06 | 0.173 | 3.74E-06 | 1.16E-04 |
| cg24409442 | 17 | 10521903 | MYHAS | Body | | MYH3 | -0.087 | 0.916 | 2.88E-06 | 8.41E-07 | -0.084 | 1.24E-04 | 3.85E-03 |
| cg07615111 | 13 | 114965537 | | | Island | CDC16 | -0.032 | 0.968 | 3.11E-06 | 9.15E-07 | -0.036 | 1.97E-05 | 6.10E-04 |
| cg11993828 | 4 | 38525620 | LINC01258 | TSS1500 | | KLF3 | 0.088 | 1.092 | 3.14E-06 | 4.34E-06 | 0.084 | 2.40E-04 | 7.43E-03 |
| cg09667394 | 1 | 78011748 | AK5 | Body | | ZZZ3 | 0.119 | 1.126 | 3.73E-06 | 5.16E-06 | 0.118 | 2.00E-04 | 6.21E-03 |
| cg14266032 | 15 | 71976359 | THSD4 | Body | | NR2E3 | -0.241 | 0.785 | 3.78E-06 | 1.13E-06 | -0.200 | 9.12E-04 | 2.83E-02 |
| cg10954740 | 8 | 110982709 | KCNV1 | Body | N_Shelf | KCNV1 | 0.112 | 1.119 | 4.20E-06 | 5.80E-06 | 0.137 | 3.54E-06 | 1.10E-04 |
| cg17463352 | 15 | 36337249 | | | | DPH6 | 0.085 | 1.088 | 4.39E-06 | 6.08E-06 | 0.087 | 1.05E-04 | 3.26E-03 |
| cg03098577 | 3 | 105516800 | CBLB | Body | | CBLB | 0.077 | 1.080 | 4.86E-06 | 6.72E-06 | 0.086 | 1.10E-04 | 3.40E-03 |
| cg04394336 | 20 | 17543720 | BFSP1 | ExonBnd | | DSTN | 0.124 | 1.132 | 4.94E-06 | 6.84E-06 | 0.133 | 5.56E-05 | 1.72E-03 |
| cg13834932 | 5 | 6373419 | MED10 | Body | | MED10 | -0.108 | 0.897 | 4.99E-06 | 1.51E-06 | -0.099 | 6.59E-05 | 2.04E-03 |
| cg27115863 | 22 | 37921640 | | | | CARD10 | 0.112 | 1.118 | 5.21E-06 | 7.21E-06 | 0.097 | 1.56E-03 | 4.84E-02 |
| cg05344747 | 11 | 33754357 | CD59 | 5'UTR | N_Shelf | CD59 | 0.089 | 1.093 | 5.80E-06 | 8.03E-06 | 0.081 | 1.56E-04 | 4.82E-03 |
| cg02462015 | 4 | 90204565 | GPRIN3 | 5'UTR | | TIGD2 | 0.059 | 1.061 | 5.80E-06 | 8.04E-06 | 0.054 | 5.18E-04 | 1.61E-02 |
| cg08001199 | 2 | 65058570 | | | | SLC1A4 | 0.133 | 1.142 | 5.82E-06 | 8.06E-06 | 0.141 | 9.10E-05 | 2.82E-03 |
| cg17904068 | 12 | 133420801 | CHFR | Body | S_Shelf | GOLGA3 | -0.450 | 0.638 | 6.61E-06 | 2.05E-06 | -0.519 | 3.52E-06 | 1.09E-04 |
| cg20583743 | 1 | 223071401 | DISP1 | 5'UTR | | DISP1 | 0.055 | 1.056 | 6.90E-06 | 9.56E-06 | 0.051 | 7.12E-04 | 2.21E-02 |
| cg19821297 | 19 | 12890029 | | | S_Shore | HOOK2 | 0.094 | 1.099 | 7.06E-06 | 9.78E-06 | 0.085 | 8.44E-04 | 2.62E-02 |

| | | | | | | | | | | | | |
|---|---|---|---|---|---|---|---|---|---|---|---|---|
| cg17852841 | 17 | 7401439 | POLR2A | Body | POLR2A | -0.350 | 0.705 | 7.17E-06 | 2.23E-06 | -0.416 | 1.09E-03 | 3.39E-02 |
| cg14088282 | 1 | 222003220 | | | DUSP10 | 0.057 | 1.059 | 7.49E-06 | 1.04E-05 | 0.055 | 5.16E-04 | 1.60E-02 |
| cg06779591 | 3 | 26410624 | | | LRRC3B | 0.116 | 1.123 | 8.38E-06 | 1.16E-05 | 0.141 | 1.43E-05 | 4.43E-04 |
| cg09584249 | 12 | 26425003 | | | SSPN | 0.090 | 1.094 | 8.42E-06 | 1.17E-05 | 0.092 | 1.42E-04 | 4.40E-03 |
| cg12866551 | 10 | 20019641 | | | PLXDC2 | 0.071 | 1.073 | 9.40E-06 | 1.30E-05 | 0.065 | 6.44E-04 | 2.00E-02 |

**Table 2.** Differentially methylated positions (DMPs) associated with vasospasm incidence in the Cox Regression Model adjusted for age, sex, smoking habit, ethnicity and Fisher scale. In this table, we show the 31 DMPs with *p*-value < $10^{-5}$. Gene annotations (first set of columns) have been obtained according to Illumina manifest (hg38) and GREAT software. Second set of columns shows the effect of the CpG on the risk of vasospasm: β-coefficients, Hazard ratios (HR) by 1% increase in methylation of the CpG and *p*-values with (Bacon) and without test-statistic inflation adjustment. Third set of columns shows the results of the sensitivity analysis excluding cases with symptom onset exceeding 48 hours.

*Keywords:* BP: base-pair; CHR: chromosome; HR, Hazard ratio.

To account for influential cases, we ran a bootstrap analysis, observing that all CpG candidates remained significant (supplementary figure 3). Similarly, as showed in table 2, we used Bacon method to adjust for test-statistic inflation, finding that 27 out of 31 DMPs remained significant (supplementary figure 4 and table 2). Finally, we ran a sensitivity analysis in this set of 31 DMPs considering only subjects with less than 48 hours of evolution since aSAH onset, finding that all CpG candidates were significantly associated with incidence of vasospasm after adjusting for multiple testing (table 2). We then checked whether these CpGs were associated with main risk factors of vasospasm. Interestingly, we observed that methylation levels of 6 CpGs were negatively correlated with age after accounting for multiple testing. Similarly, other DMPs were associated with risk factors of vasospasm such as sex, history of hypertension or smoking (figure 2).

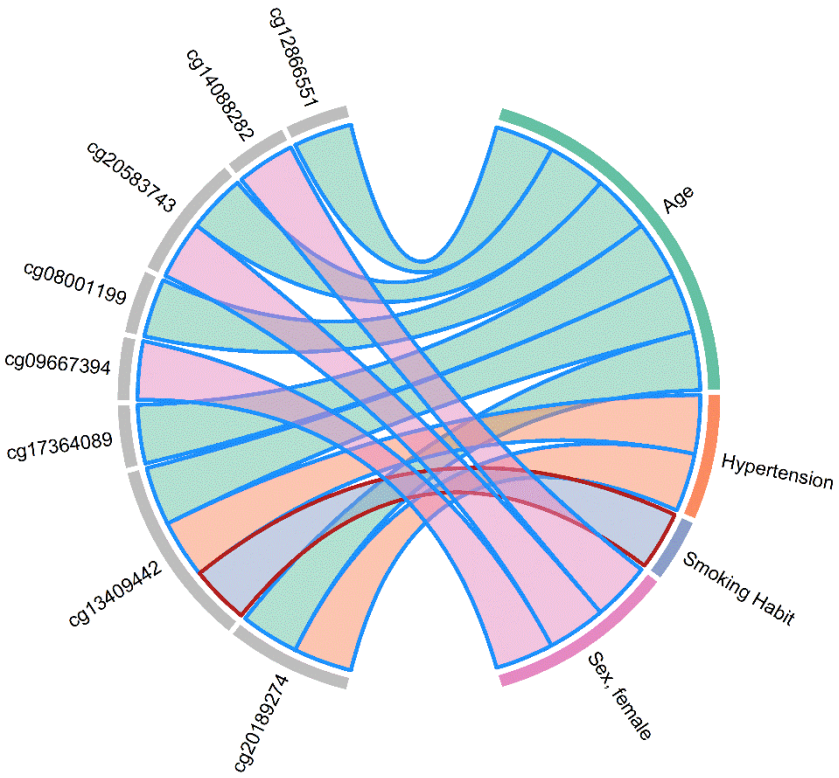


**Figure 2** Association between significant DMPs (p-value < 10-5) and main clinical factors. This plot represents the relationship between methylation levels of nominally significant DMPs and main clinical factors associated with vasospasm. Links between CpGs (left side) and clinical variables (right side) indicate significant associations. Border links correspond to whether we see a positive or negative correlation (red and blue colors, respectively). Filling colors correspond to clinical factors as labeled on the right side of the figure. Hypermethylation at these sites was associated with risk of vasospasm (table 2)

*Keywords: DMP, differentially methylated positions; SAH, subarachnoid hemorrhage*.

**Differentially methylated regions analysis**

After correcting for multiple testing, we found 13 DMR associated with vasospasm (table 3). Among them, four regions included 10 or more CpGs associated with vasospasm annotated to the following genes: POU Class 5 Homeobox 1 (*POU5F1*), Major Histocompatibility Complex Class II DP Alpha 1 (*HLA-DPA1*), RUN and FYVE Domain Containing 1 (*RUFY1*) and Cytochrome P450 Family 1 Subfamily A Member 1 (*CYP1A1*). Figure 3-top panel visually illustrates these four DMRs, revealing that two are situated within promoter regions while one is located within the gene body. No information was available for the last DMR based on the Illumina manifest. The comparison of methylation levels of the top CpG candidates for each region showed that three DMRs were hypermethylated in patients with vasospasm, while one of them (annotated to *RUFY* gene) was hypomethylated and located in a promotor region (figure 3-bottom panel). Moreover, when we averaged the methylation level of CpGs included in the 13 significant DMRs, we observed that most DMRs were hypermethylated in patients with vasospasm, as we observed before for DMPs (supplementary figure 5). We finally studied the relationship between averaged methylation for each DMR and main risk factors (Supplementary figure 6). Interestingly, most regions showed at least one significant association with clinical factors. There were three regions hypermethylated in females (*POU5F1, CYP1A1* and Sarcospan [*SSPN*] genes) and two hypermethylated in males (*RUFY1* and Charged Multivesicular Body Protein 6 [*CHMP6*] genes).

**Table 3. Differentially Methylated Regions in patients with Vasospasm**

| Chromosome | Start | End | *p*-value | Q-value | CpGs N | Gene (GREAT annotation) |
|---|---|---|---|---|---|---|
| CHR6 | 31180555 | 31180890 | 5.73E-14 | 6.87E-13 | 14 | POU5F1 |
| CHR6 | 33116777 | 33117287 | 6.09E-12 | 3.65E-11 | 14 | HLA-DPA1 |
| CHR5 | 179559290 | 179559906 | 5.12E-16 | 1.23E-14 | 13 | RUFY1 |
| CHR15 | 74726729 | 74727036 | 2.80E-09 | 7.14E-09 | 10 | CYP1A1 |
| CHR6 | 28977412 | 28977731 | 1.26E-08 | 2.15E-08 | 7 | ZNF311 |
| CHR12 | 26271763 | 26272279 | 4.16E-12 | 3.33E-11 | 6 | SSPN |
| CHR3 | 16174538 | 16174709 | 1.18E-10 | 5.64E-10 | 6 | GALNT15 |
| CHR5 | 178443176 | 178443407 | 1.40E-07 | 1.86E-07 | 6 | COL23A1 |
| CHR1 | 24112213 | 24112586 | 2.98E-09 | 7.14E-09 | 5 | MYOM3 |
| CHR1 | 165544016 | 165544125 | 7.31E-09 | 1.35E-08 | 5 | LRRC52 |
| CHR9 | 97039709 | 97039758 | 8.82E-10 | 3.02E-09 | 4 | CTSV |
| CHR2 | 23617398 | 23617686 | 6.16E-09 | 1.34E-08 | 4 | KLHL29 |
| CHR17 | 80891568 | 80891863 | 6.28E-08 | 9.42E-08 | 4 | CHMP6 |

**Table 3.** Each region is annotated according to the chromosome, start-end base pairs and gene (GREAT software). Significance levels have been obtained via *comb-p* library, using EWAS summary statistics as input. We also show significance after adjusting for multiple testing (Sidak correction) and number of CpGs conforming the region. We only considered regions having at least 4 CpGs.

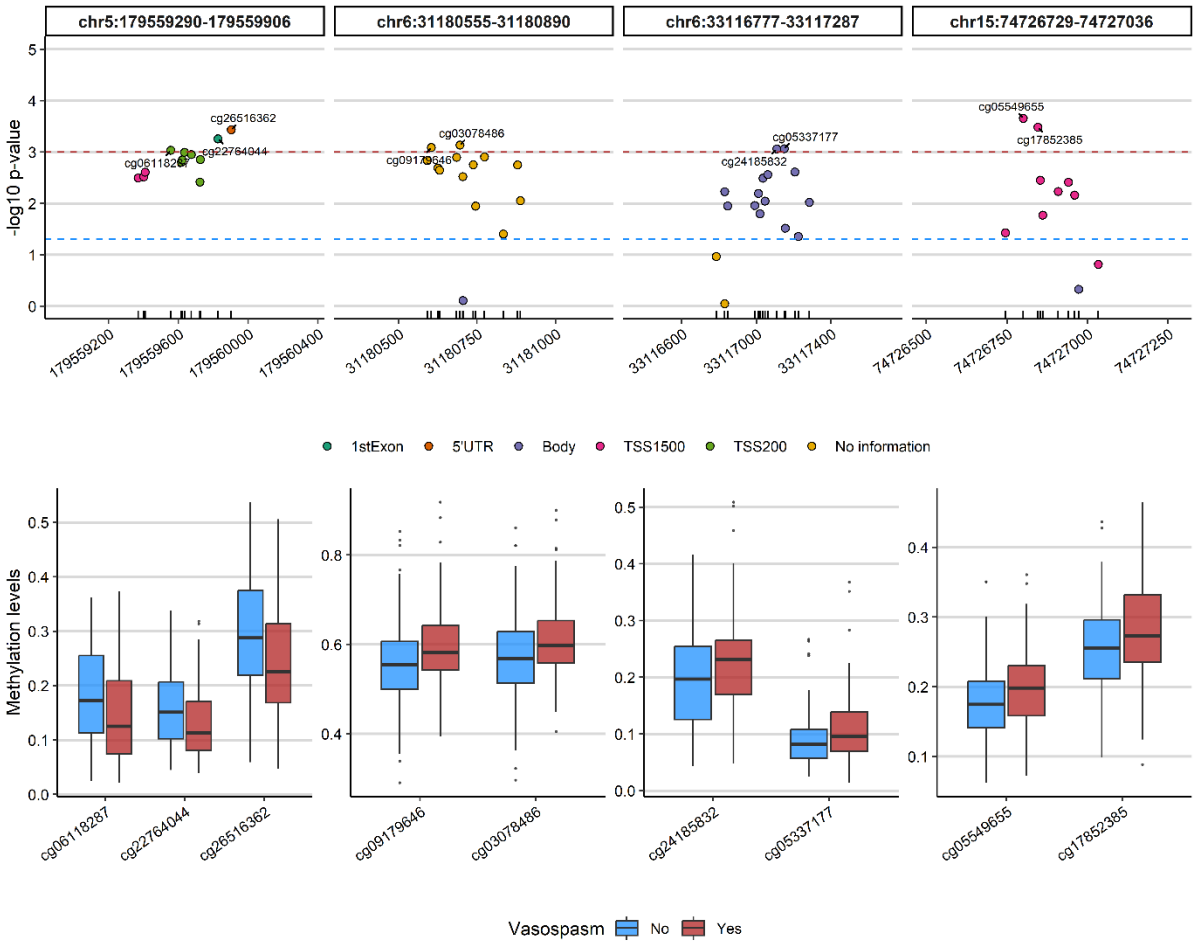


**Figure 3** Top differentially methylated regions (DMR) associated with incidence of vasospasm. We found 4 DMRs significant at Q-value < 0.05 and being conformed by more than 10 CpGs. In the top panel we show the CpGs within each DMR according to the -log10 p-value (Y axis) and genomic coordinates (X axis, Hg38). Dots have been filled according to the location of each CpG relative to the gene. The red dashed line corresponds to the significance level for the seed p-value (see the methods section), while the blue line corresponds to the nominal significance level. In the bottom panel we compare the methylation levels of those CpGs above the seed p-value for each DMR

*Keywords: TSS, transcriptomic start site.*

## Pathway analysis

We conducted a ranked gene set enrichment analysis leveraging GO, KEGG and Reactome databases. After applying FDR correction, we found 9 significant GO pathways and 39 Reactome pathways (Supplementary table 2). We found pathways related to immunity, inflammatory response, nervous system, extracellular matrix organization, oxidative stress, and apoptosis. We calculated the similarity between the significant pathways to infer which broad biological functions were enriched in our experiment, aiming to summarize the results. We then built and acyclic graph where nodes were gene-sets, either annotated to GO or Reactome, and edges represented the number of genes in common between them (Supplementary figure 7). Thereby, we found that gene-sets clustered onto biological functions such as glycogen metabolism, nervous system, regulation of Tumor Protein 53 (*TP53*) and inflammation.

## DISCUSSION

This study marks a pioneering effort in assessing the impact of DNAm on the occurrence of vasospasm. Our findings reveal at least one DMP and thirteen DMRs linked to this complication, with some of them annotated to genes known to participate in biological mechanisms previously associated with vasospasm. Notably, our pathway analysis unveiled an enrichment of significant biological processes, including the inflammatory response, extracellular matrix organization, and apoptosis, shedding light on potential molecular pathways contributing to the development of vasospasm.

Our study is the largest to date that analyzes DNAm in the blood of aSAH patients. While two previous studies have analyzed the association of DNAm with the incidence of DCI, none of them have explored vasospasm[38,39]. Specifically, one study confirmed associations between methylation at the Insulin receptor (*INSR*) and Cadherin Related Family Member 5 (*CDHR5*) genes with DCI[39]. However, an additional study failed to demonstrate a significant effect of *ANGPT1* methylation on DCI risk, highlighting the complexities of epigenetic contributions on aSAH complications and the need for further research[38]. Moreover, the association of vasospasm and DCI is complex. Vasospasm increases the risk of DCI, a major prognostic determinant[3]. However, the etiology of DCI extends beyond vasospasm[40]. In our study, although 38.6% of patients experiencing vasospasm developed DCI, a substantial 10.9% of those without vasospasm also suffered from DCI. Therefore, DCI cannot be solely attributed to vasospasm and it may help to explain why our findings have not been previously reported in studies focused on DCI.

We found 31 CpGs associated with vasospasm at the nominal significance level, being cg26189827 (*SUGCT* gene) the only CpG significant at the genome-wide level. This gene encodes a protein that catalyzes the succinyl-CoA-dependent conversion of glutarate to glutaryl-CoA and it is mainly expressed in the arterial tissue according to GTEx Portal, but its ultimate physiological role is unknown. Variants in this gene have been previously associated with glutaric aciduria[41,42] type 3, a rare metabolic disease characterized by isolated glutaric acid excretion. In some patients, neurological findings such as microcephaly, hypotonia or neuromotor delay are present[43–45]. Moreover, a case report showed white matter abnormalities with sparing of the U fibers of the cerebral hemispheres probably due to neurovascular alterations[43]. In that sense, variants in *SUGCT* gene have also been associated with pulse pressure and increased risk of migraine in GWAS studies[46–48]contributing to its role in vascular functionality. Interestingly, previous research posed that artery stiffness and elasticity could contribute to the risk of vasospasm[49,50], suggesting that the diminished elasticity observed in older patient's vessel walls might underlie their reduced susceptibility to its development. On the other hand, mechanisms such as vasoconstriction of cerebral arterioles and cortical spreading depression are implicated in the pathophysiology of both migraine and cerebral vasospasm.

Furthermore, individuals with migraine, particularly young women, exhibit an increased risk of DCI[51,52]. However, the association between migraine and vasospasm has not been thoroughly explored. Therefore, we believe that further clinical studies are necessary to investigate the role of SUGCT in the pathogenesis of both vasospasm and migraine, as well as to elucidate the link between these two conditions.

Similarly, we found other interesting genes annotated to our nominally significant DMPs, such as the DNA Polymerase Kappa (*POLK*), NADPH Oxidase 5 (*NOX5*) and Mitogen-Activated Protein Kinase Kinase Kinase Kinase 5 (*MAP4K5*). *POLK* is involved in susceptibility to oxidative damage, a mechanism that has already been associated with vasospasm development[53]. *NOX5* participates in endothelial oxidative stress and seems to play a role in the regulation of vascular contraction[54], endothelial proliferation, angiogenesis and endothelial response to thrombin[55]. Finally, *MAP4K5*, a constituent of the Mitogen-Activated Protein Kinases (MAPKs) family, contributes to vasospasm's pathogenesis due to its involvement in the contraction of vascular smooth muscle cells, and previous studies have indicated that the inhibition of MAPKs could potentially mitigate this complication[56,57].

Many CpGs in vasospasm patients showed increased methylation, especially in younger individuals. Although the influence of age on vasospasm is not completely understood[50,58], we found a higher risk in younger patients and, in line with this result, several CpG that were nominally significant were negatively correlated with age. These results agree with our previous work where we found a higher risk of vasospasm in cases with decreased biological age measured through DNAm epigenetic clocks[59]. This points again to specific epigenetic mechanisms being implicated in the pathophysiology of vasospasm associated with aging.

We further investigated the relationship between these CpGs and the risk factors for vasospasm. Our analysis revealed variations in methylation patterns associated with female sex, smoking habits and history of hypertension, confirming the epigenetic signatures of these factors. The role of hypertension as a vasospasm risk factor is not clear, although most studies found no association[25]. In our study, there was no difference in history of hypertension between vasospasm and no-vasospasm groups, but we observed that two nominally significant CpGs were also associated with presence of hypertension. However, this effect is likely confounded by the effect of aging both on hypertension and methylation at these sites. On the other hand, smoking habit is known to increase the risk of vasospasm[25], and cg13409442 also related to this trait, being the direction of the effect congruent with the results obtained in our EWAS of vasospasm.

We then examined whether there were genomic regions exhibiting differential methylation in patients with vasospasm. Consequently, we identified 13 significant DMRs, with four of them comprising ten or more CpG positions. These DMRs were annotated to the following genes: *POU5F1, HLA-DPA1, RUFY1*, and *CYP1A1*. As we observed for DMP analyses, most of these regions were hypermethylated in patients with vasospasm, except the region annotated to *RUFY1*, which was hypomethylated. This DMR is located near the transcriptomic start site, suggesting that patients with vasospasm have a higher expression of this gene as compared to patients without[4]. This candidate is involved in endosomal trafficking and previous research found that its coding protein is involved in late onset Alzheimer's disease[60]. Moreover, we observed that male sex was related to hypomethylation at *RUFY1* and there were 4 additional DMRs associated with sex, being three of them hypermethylated in females. These findings imply that certain DMRs may exhibit distinct methylation signals based on sex. This encourages additional investigations into how sex modulates the epigenetic signature of vasospasm, especially considering the documented sex-related differences in the risk of aSAH and its complications[61]. Regarding *CYP1A1*, recognized as a metabolizing enzyme, possesses the capability to metabolize certain carcinogenic intermediates found in cigarettes, a correlation linked to lung cancer[62]. Additionally, it has been investigated in the context of ischemic stroke, where a polymorphism is associated with a reduced risk[63]. On the other hand, *POU5F1*, also known as OCT4, is a transcription factor that plays an important role in embryonic development and stem cell pluripotency[64]. Although there are no studies relating it to aSAH or vasospasm, it has been associated with tumorgenesis[65] and it has been found upregulated after hypoxia in glioma cells[66]. With regard to HLA-DPA1, this specific HLA type has not been previously reported in association with aSAH, but other HLA subtypes have been linked to the occurrence of brain and abdominal aortic aneurysms, as well as outcomes following aSAH, though the underlying mechanisms remain incompletely understood[67].

Finally, our gene-set enrichment analysis revealed compelling candidate mechanisms linked to vasospasm. Notably, we observed a significant enrichment of gene-sets related to the inflammatory response, including interleukine-3 and 5 signaling. Robust evidence supports the role of pro-inflammatory response in the onset and maintenance of vasospasm after aSAH[40,68], as evidenced by increased expression of inflammatory biomarkers such as C-reactive protein or leukocyte count[69,70]. Likewise, we found an overrepresentation of the extracellular matrix organization pathway, which has been involved in patients with vasospasm, through an upregulation of extracellular matrix proteins such as the Matrix Metalloproteinase-9[71–73], because of an increased blood-brain barrier permeability and oxidative stress during vasospasm development[68]. Lastly, we also found an enrichment in several gene-sets related to *TP53*, which is a key regulator of apoptosis that has been involved in early brain injury after aSAH[74,75]. It is important to highlight that our

enrichment results might not necessarily indicate causal mechanism of vasospasm and could potentially be consequences or simply epiphenomena.

Given the lack of studies on DNAm and vasospasm, we also compared our results with those from investigations analyzing the gene expression patterns in blood from patients with vasospasm and aSAH. Interestingly, one transcriptomic study found that Formin-Like Protein 3 (*FMNL3*), Beaded Filament Structural Protein 1 (*BFSP1*) and Hook Microtubule Tethering Protein 2 (*HOOK2*) were differentially expressed in patients with vasospasm and aSAH[76]. Moreover, previous research has found enrichment in analogous biological functions, including immunity and inflammation[76,77], oxidative stress[76,78], and extracellular matrix organization[71]. These studies, however, are limited both in number and sample size, and further investigations measuring both DNAm and gene expression would be required to understand how methylation affects the risk of vasospasm.

Our study exhibits both limitations and strengths. A noteworthy limitation is the absence of result replication in an independent cohort, underscoring the hypothesis-generating aspect of our findings, which necessitates further validation. We have attempted to find a replication cohort but have not succeeded in finding studies that include the necessary information. Additionally, despite boasting the largest sample size for a study of this kind, there remains a possibility that it may be inadequate for detecting additional associations. Nonetheless, this does not diminish the significance of the established associations. Finally, a repeated limitation in epigenetic studies is the use of whole-blood samples to estimate DNAm of other organs or tissues. Nevertheless, previous studies have shown a good correlation between DNAm from blood, brain and arterial tissue[79,80], but depending on specific loci. Moreover, blood samples are the most readily accessible in clinical practice, making the analysis of blood biomarkers an ideal choice for translational medicine. Conversely, the main strength of the study lies in its novelty, being the first EWAS addressed to vasospasm and the first to propose a potential influence of DNAm on the susceptibility to this complication. Furthermore, the dataset originates from a thoroughly phenotyped cohort, meticulously accounting for confounding factors and incorporating several epigenetic approaches including DMPs, DMRs and pathway enrichment. In the end, a rigorous bias assessment has been considered at every stage of the analysis.

In conclusion, our study unveils for the first time a distinctive DNAm pattern in patients experiencing vasospasm following aSAH. We found a significant association with a CpG position annotated to the SUGCT gene, which is expressed in arterial tissue, among several other candidate genes related to the vascular function. The analysis of epigenetic regions and gene enrichment uncovered compelling associations with genes and pathways integral to inflammatory and immune responses, extracellular matrix organization, apoptosis and susceptibility to oxidative damage. Notably, the DNAm profile demonstrated influences from both sex and age, underscoring the significance of these factors in the

pathogenesis of vasospasm. These findings open avenues for further investigation to corroborate our results, offering potential insights into the underlying pathophysiology of this prevalent and serious complication.

**Data Availability:** Data supporting the findings of this study are available upon reasonable request.

## REFERENCES

1. Lo BWY, Fukuda H, Nishimura Y, Farrokhyar F, Thabane L, Levine MAH. Systematic review of clinical prediction tools and prognostic factors in aneurysmal subarachnoid hemorrhage. Surg Neurol Int. 2015;6.
2. Lantigua H, Ortega-Gutierrez S, Schmidt JM, Lee K, Badjatia N, Agarwal S, et al. Subarachnoid hemorrhage: Who dies, and why? Crit Care. 2015;19.
3. Chalet FX, Briasoulis O, Manalastas EJ, Talbot DA, Thompson JC, Macdonald RL. Clinical Burden of Angiographic Vasospasm and Its Complications After Aneurysmal Subarachnoid Hemorrhage: A Systematic Review. Neurol Ther. Adis; 2023. p. 371–90.
4. Portela A, Esteller M. Epigenetic modifications and human disease. Nat Biotechnol. 2010. p. 1057–68.
5. Soriano-Tárraga C, Lazcano U, Giralt-Steinhauer E, Avellaneda-Gómez C, Ois Á, Rodríguez-Campello A, et al. Identification of 20 novel loci associated with ischaemic stroke. Epigenome-wide association study. Epigenetics. 2020;15:988–97.
6. Zhang Y, Long H, Wang S, Xiao W, Xiong M, Liu J, et al. Genome-Wide DNA Methylation Pattern in Whole Blood Associated With Primary Intracerebral Hemorrhage. Front Immunol. 2021;12.
7. Solodovnikova Y, Ivaniuk A, Marusich T, Son A. Meta-analysis of associations of genetic polymorphisms with cerebral vasospasm and delayed cerebral ischemia after aneurysmal subarachnoid hemorrhage. Acta Neurol Belg [Internet]. 2022 [cited 2024 Mar 26];122:1547–56. Available from: https://pubmed.ncbi.nlm.nih.gov/34725794/
8. Heinsberg LW, Arockiaraj AI, Crago EA, Ren D, Shaffer JR, Sherwood PR, et al. Genetic Variability and Trajectories of DNA Methylation May Support a Role for HAMP in Patient Outcomes After Aneurysmal Subarachnoid Hemorrhage. Neurocrit Care [Internet]. 2020 [cited 2024 Mar 26];32:550–63. Available from: https://pubmed.ncbi.nlm.nih.gov/31346934/
9. Heinsberg LW, Weeks DE, Alexander SA, Minster RL, Sherwood PR, Poloyac SM, et al. Iron homeostasis pathway DNA methylation trajectories reveal a role for STEAP3 metalloreductase in patient outcomes after aneurysmal subarachnoid hemorrhage. Epigenetics communications [Internet]. 2021 [cited 2024 Mar 26];1. Available from: https://pubmed.ncbi.nlm.nih.gov/35083470/
10. Jung CS. Nitric oxide synthase inhibitors and cerebral vasospasm. Acta Neurochir Suppl [Internet]. 2011 [cited 2024 Mar 26];110:87–91. Available from: https://pubmed.ncbi.nlm.nih.gov/21116921/
11. Medina-Suárez J, Rodríguez-Esparragón F, Sosa-Pérez C, Cazorla-Rivero S, Torres-Mata LB, Jiménez-O'Shanahan A, et al. A Review of Genetic Polymorphisms and Susceptibilities to Complications after Aneurysmal Subarachnoid Hemorrhage. Int J Mol Sci [Internet]. 2022 [cited 2024 Mar 26];23. Available from: https://pubmed.ncbi.nlm.nih.gov/36499752/

12. Wei S, Tao J, Xu J, Chen X, Wang Z, Zhang N, et al. Ten Years of EWAS. Advanced Science. John Wiley and Sons Inc; 2021.
13. Fernandez-Perez I, Giralt-Steinhauer E, Cuadrado-Godia E, Guimaraens L, Vivas E, Saldaña J, et al. Long-term vascular events after subarachnoid hemorrhage. Journal of Neurology. 2022;269:6036–42.
14. Roquer J, Cuadrado-Godia E, Guimaraens L, Conesa G, Rodríguez-Campello A, Capellades J, et al. Short-and long-term outcome of patients with aneurysmal subarachnoid hemorrhage. Neurology. 2020;95:E1819–29.
15. Treggiari MM, Rabinstein AA, Busl KM, Caylor MM, Citerio G, Deem S, et al. Guidelines for the Neurocritical Care Management of Aneurysmal Subarachnoid Hemorrhage. Neurocrit Care. 2023;
16. Vivancos J, Gilo F, Frutos R, Maestre J, García-Pastor A, Quintana F, et al. Clinical management guidelines for subarachnoid haemorrhage. Diagnosis and treatment. Neurologia. Spanish Society of Neurology; 2014. p. 353–70.
17. Dedeurwaerder S, Defrance M, Bizet M, Calonne E, Bontempi G, Fuks F. A comprehensive overview of Infinium Human Methylation450 data processing. Brief Bioinform. 2013;15:929–41.
18. Aryee MJ, Jaffe AE, Corrada-Bravo H, Ladd-Acosta C, Feinberg AP, Hansen KD, et al. Minfi: a flexible and comprehensive Bioconductor package for the analysis of Infinium DNA methylation microarrays. Bioinformatics [Internet]. 2014;30:1363–9. Available from: https://doi.org/10.1093/bioinformatics/btu049
19. Chen YA, Lemire M, Choufani S, Butcher DT, Grafodatskaya D, Zanke BW, et al. Discovery of cross-reactive probes and polymorphic CpGs in the Illumina Infinium HumanMethylation450 microarray. Epigenetics. 2013;8:203–9.
20. Zhou W, Laird PW, Shen H. Comprehensive characterization, annotation and innovative use of Infinium DNA methylation BeadChip probes. Nucleic Acids Res. 2017;45:e22.
21. Teschendorff AE, Marabita F, Lechner M, Bartlett T, Tegner J, Gomez-Cabrero D, et al. A beta-mixture quantile normalization method for correcting probe design bias in Illumina Infinium 450 k DNA methylation data. Bioinformatics. 2013;29:189–96.
22. Leek JT, Johnson WE, Parker HS, Fertig EJ, Jaffe AE, Zhang Y, Storey JD TL. sva: Surrogate Variable Analysis. R package version 3420. 2021;
23. Houseman EA, Accomando WP, Koestler DC, Christensen BC, Marsit CJ, Nelson HH, et al. DNA methylation arrays as surrogate measures of cell mixture distribution. BMC Bioinformatics. 2012;13.
24. McLean CY, Bristor D, Hiller M, Clarke SL, Schaar BT, Lowe CB, et al. GREAT improves functional interpretation of cis-regulatory regions. Nat Biotechnol. 2010;28:495–501.
25. Inagawa T. Risk Factors for Cerebral Vasospasm Following Aneurysmal Subarachnoid Hemorrhage: A Review of the Literature. World Neurosurg. 2016;85:56–76.
26. Rumalla K, Lin M, Ding L, Gaddis M, Giannotta SL, Attenello FJ, et al. Risk Factors for Cerebral Vasospasm in Aneurysmal Subarachnoid Hemorrhage: A Population-Based Study of 8346 Patients. World Neurosurg. 2021;145:e233–41.
27. Kader F, Ghai M. DNA methylation-based variation between human populations. Molecular Genetics and Genomics. Springer Verlag; 2017. p. 5–35.
28. Joehanes R, Just AC, Marioni RE, Pilling LC, Reynolds LM, Mandaviya PR, et al. Epigenetic Signatures of Cigarette Smoking. Circ Cardiovasc Genet. 2016;9:436–47.
29. Jones MJ, Goodman SJ, Kobor MS. DNA methylation and healthy human aging. Aging Cell. Blackwell Publishing Ltd; 2015. p. 924–32.
30. Carter A, Bares C, Lin L, Reed BG, Bowden M, Zucker RA, et al. Sex-specific and generational effects of alcohol and tobacco use on epigenetic age acceleration in the Michigan longitudinal study. Drug and Alcohol Dependence Reports. 2022;4:100077.

31. van Iterson M, van Zwet EW, Heijmans BT, 't Hoen PAC, van Meurs J, Jansen R, et al. Controlling bias and inflation in epigenome- and transcriptome-wide association studies using the empirical null distribution. Genome Biol. 2017;18.
32. Pedersen BS, Schwartz DA, Yang I V., Kechris KJ. Comb-p: Software for combining, analyzing, grouping and correcting spatially correlated P-values. Bioinformatics. 2012;28:2986–8.
33. Li QS, Sun Y, Wang T. Epigenome-wide association study of Alzheimer's disease replicates 22 differentially methylated positions and 30 differentially methylated regions. Clin Epigenetics. 2020;12:149.
34. Zhang L, Silva TC, Young JI, Gomez L, Schmidt MA, Hamilton-Nelson KL, et al. Epigenome-wide meta-analysis of DNA methylation differences in prefrontal cortex implicates the immune processes in Alzheimer's disease. Nat Commun [Internet]. 2020;11. Available from: http://dx.doi.org/10.1038/s41467-020-19791-w
35. Lawrence M, Huber W, Pagès H, Aboyoun P, Carlson M, Gentleman R, et al. Software for Computing and Annotating Genomic Ranges. PLoS Comput Biol. 2013;9:1–10.
36. Martin TC, Yet I, Tsai PC, Bell JT. coMET: Visualisation of regional epigenome-wide association scan results and DNA co-methylation patterns. BMC Bioinformatics. 2015;16.
37. Ren X, Kuan PF. methylGSA: a Bioconductor package and Shiny app for DNA methylation data length bias adjustment in gene set testing. Bioinformatics. 2019;35:1958–9.
38. Liu D, Arockiaraj AI, Shaffer JR, Poloyac SM, Sherwood PR, Alexander SA, et al. ANGPT1 methylation and delayed cerebral ischemia in aneurysmal subarachnoid hemorrhage patients. Epigenetics Communications. 2021;1:1–20.
39. Kim BJ, Kim Y, Youn DH, Park JJ, Rhim JK, Kim HC, et al. Genome-wide blood DNA methylation analysis in patients with delayed cerebral ischemia after subarachnoid hemorrhage. Sci Rep. 2020;10:11419.
40. Dodd WS, Laurent D, Dumont AS, Hasan DM, Jabbour PM, Starke RM, et al. Pathophysiology of delayed cerebral ischemia after subarachnoid hemorrhage: A review. J Am Heart Assoc. American Heart Association Inc.; 2021.
41. Waters PJ, Kitzler TM, Feigenbaum A, Geraghty MT, Al-Dirbashi O, Bherer P, et al. Glutaric Aciduria Type 3: Three Unrelated Canadian Cases, with Different Routes of Ascertainment. 2017. p. 89–96.
42. Sherman EA, Strauss KA, Tortorelli S, Bennett MJ, Knerr I, Morton DH, et al. Genetic Mapping of Glutaric Aciduria, Type 3, to Chromosome 7 and Identification of Mutations in C7orf10. The American Journal of Human Genetics. 2008;83:604–9.
43. Dorum S, Havalı C, Görükmez Ö, Görükmez O. Two patients with glutaric aciduria type 3: a novel mutation and brain magnetic resonance imaging findings. Turk J Pediatr. 2020;62:657.
44. Demir E, Doğulu N, Tuna Kırsaçlıoğlu C, Topçu V, Eminoglu FT, Kuloğlu Z, et al. A Rare Contiguous Gene Deletion Leading to Trichothiodystrophy Type 4 and Glutaric Aciduria Type 3. Mol Syndromol. 2023;14:136–42.
45. La Serna-Infantes J, Pastor MC, Trubnykova M, Velásquez FC, Sotomayor FV, Barriga HA. Novel contiguous gene deletion in peruvian girl with Trichothiodystrophy type 4 and glutaric aciduria type 3. Eur J Med Genet. 2018;61:388–92.
46. Sollis E, Mosaku A, Abid A, Buniello A, Cerezo M, Gil L, et al. The NHGRI-EBI GWAS Catalog: knowledgebase and deposition resource. Nucleic Acids Res. 2023;51:D977–85.
47. Anttila V, Winsvold BS, Gormley P, Kurth T, Bettella F, McMahon G, et al. Genome-wide meta-analysis identifies new susceptibility loci for migraine. Nat Genet [Internet]. 2013 [cited 2023 Jun 23];45:912. Available from: /pmc/articles/PMC4041123/

48. Warren HR, Evangelou E, Cabrera CP, Gao H, Ren M, Mifsud B, et al. Genome-wide association analysis identifies novel blood pressure loci and offers biological insights into cardiovascular risk. Nat Genet. 2017;49:403–15.
49. Claus JJ, Breteler MMB, Hasan D, Krenning EP, Bots ML, Grobbee DE, et al. Regional cerebral blood flow and cerebrovascular risk factors in the elderly population. Neurobiol Aging [Internet]. 1998 [cited 2023 Jun 26];19:57–64. Available from: https://pubmed.ncbi.nlm.nih.gov/9562504/
50. Torbey MT, Hauser K, Bhardwaj A, Williams MA, Ulatowski JA, Mirski MA, et al. Effect of Age on Cerebral Blood Flow Velocity and Incidence of Vasospasm After Aneurysmal Subarachnoid Hemorrhage [Internet]. 2001. Available from: http://ahajournals.org
51. van Os HJA, Ruigrok YM, Verbaan D, Dennesen P, Müller MCA, Coert BA, et al. Delayed Cerebral Ischemia After Aneurysmal Subarachnoid Hemorrhage in Patients With a History of Migraine. Stroke. 2020;51:3039–44.
52. Ellis JA, Goldstein H, Meyers PM, Lavine SD, Connolly ES, Mayer SA, et al. Post-subarachnoid Hemorrhage Vasospasm in Patients with Primary Headache Disorders. Neurocrit Care. 2013;18:362–7.
53. Yang Y, Chen S, Zhang J-M. The Updated Role of Oxidative Stress in Subarachnoid Hemorrhage. Curr Drug Deliv [Internet]. 2017 [cited 2023 Jun 23];14. Available from: https://pubmed.ncbi.nlm.nih.gov/27784210/
54. Touyz RM, Anagnostopoulou A, Rios F, Montezano AC, Camargo LL. NOX5: Molecular biology and pathophysiology. Exp Physiol. Blackwell Publishing Ltd; 2019. p. 605–16.
55. BelAiba RS, Djordjevic T, Petry A, Diemer K, Bonello S, Banfi B, et al. NOX5 variants are functionally active in endothelial cells. Free Radic Biol Med. 2007;42:446–59.
56. Suzuki H, Hasegawa Y, Kanamaru K, Zhang JH. Mitogen-activated protein kinases in cerebral vasospasm after subarachnoid hemorrhage: a review. Acta Neurochir Suppl [Internet]. 2011 [cited 2023 Jun 23];110:133–9. Available from: https://pubmed.ncbi.nlm.nih.gov/21116928/
57. Zubkov AY, Nanda A, Zhang JH. Signal transduction pathways in cerebral vasospasm [Internet]. Available from: www.elsevier.com/locate/pathophys
58. Ryttlefors M, Enblad P, Ronne-Engström E, Persson L, Ilodigwe D, Macdonald RL. Patient age and vasospasm after subarachnoid hemorrhage. Neurosurgery. 2010;67:911–7.
59. Macias-Gómez A, Jiménez-Balado J, Fernández-Pérez I, Suárez-Pérez A, Vallverdú-Prats M, Guimaraens L, et al. The influence of epigenetic biological age on key complications and outcomes in aneurysmal subarachnoid haemorrhage. J Neurol Neurosurg Psychiatry. 2024;jnnp-2023-332889.
60. Kunkle BW, Vardarajan BN, Naj AC, Whitehead PL, Rolati S, Slifer S, et al. Early-Onset Alzheimer Disease and Candidate Risk Genes Involved in Endolysosomal Transport. JAMA Neurol [Internet]. 2017 [cited 2023 Jun 26];74:1113–22. Available from: https://pubmed.ncbi.nlm.nih.gov/28738127/
61. Oppong MD, Iannaccone A, Gembruch O, Pierscianek D, Chihi M, Dammann P, et al. Vasospasm-related complications after subarachnoid hemorrhage: the role of patients' age and sex. Acta Neurochir (Wien) [Internet]. 2018 [cited 2023 Jun 26];160:1393–400. Available from: https://pubmed.ncbi.nlm.nih.gov/29704122/
62. Qihua GU, Chen F, Chen N, Wang J, Zhao LI, Deng X. Effect of EGCG on bronchial epithelial cell premalignant lesions induced by cigarette smoke and on its CYP1A1 expression. Int J Mol Med. 2021;48.
63. Karimian M, Karimnia F. CYP1A1 common gene polymorphisms and ischemic stroke risk: a meta-analysis and a structural examination. Per Med. 2023;20:271–81.
64. Yoshimatsu S, Murakami R, Sato T, Saeki T, Yamamoto M, Sasaki E, et al. Generation of a common marmoset embryonic stem cell line CMES40-OC harboring a POU5F1 (OCT4)-2A-mCerulean3 knock-in reporter allele. Stem Cell Res. 2021;53:102308.

65. Stelzer G, Rosen N, Plaschkes I, Zimmerman S, Twik M, Fishilevich S, et al. The GeneCards Suite: From Gene Data Mining to Disease Genome Sequence Analyses. Curr Protoc Bioinformatics. 2016;54.
66. Qiu W, Guo X, Li B, Wang J, Qi Y, Chen Z, et al. Exosomal miR-1246 from glioma patient body fluids drives the differentiation and activation of myeloid-derived suppressor cells. Molecular Therapy. 2021;29:3449–64.
67. Frösen J, Pitkäniemi J, Tulamo R, Marjamaa J, Isoniemi H, Niemelä M, et al. Association of Fatal Aneurysmal Subarachnoid Hemorrhage with Human Leukocyte Antigens in the Finnish Population. Hum Immunol. 2007;68:100–5.
68. Av C, Voinescu D, Da N. Subarachnoid hemorrhage and cerebral vasospasm-Literature review. J Med Life.
69. McGirt MJ, Mavropoulos JC, McGirt LY, Alexander MJ, Friedman AH, Laskowitz DT, et al. Leukocytosis as an independent risk factor for cerebral vasospasm following aneurysmal subarachnoid hemorrhage. J Neurosurg [Internet]. 2003 [cited 2023 Jun 27];98:1222–6. Available from: https://pubmed.ncbi.nlm.nih.gov/12816268/
70. Rasmussen R, Bache S, Stavngaard T, Møller K. Plasma Levels of IL-6, IL-8, IL-10, ICAM-1, VCAM-1, IFNγ, and TNFα are not Associated with Delayed Cerebral Ischemia, Cerebral Vasospasm, or Clinical Outcome in Patients with Subarachnoid Hemorrhage. World Neurosurg [Internet]. 2019 [cited 2023 Jun 27];128:e1131–6. Available from: https://pubmed.ncbi.nlm.nih.gov/31121365/
71. Fischer M, Dietmann A, Beer R, Broessner G, Helbok R, Pfausler B, et al. Differential Regulation of Matrix-Metalloproteinases and Their Tissue Inhibitors in Patients with Aneurysmal Subarachnoid Hemorrhage. PLoS One. 2013;8.
72. Wang L, Gao Z. Expression of MMP-9 and IL-6 in patients with subarachnoid hemorrhage and the clinical significance. Exp Ther Med. 2018;15:1510–4.
73. McGirt MJ, Lynch JR, Blessing R, Warner DS, Friedman AH, Laskowitz DT, et al. Serum von Willebrand factor, matrix metalloproteinase-9, and vascular endothelial growth factor levels predict the onset of cerebral vasospasm after aneurysmal subarachnoid hemorrhage. Neurosurgery [Internet]. 2002 [cited 2023 Jun 27];51:1128–35. Available from: https://pubmed.ncbi.nlm.nih.gov/12383357/
74. Kuang H, Wang T, Liu L, Tang C, Li T, Liu M, et al. Treatment of early brain injury after subarachnoid hemorrhage in the rat model by inhibiting p53-induced ferroptosis. Neurosci Lett [Internet]. 2021 [cited 2023 Jun 27];762. Available from: https://pubmed.ncbi.nlm.nih.gov/34311053/
75. Yang S, Tang W, He Y, Wen L, Sun B, Li S. Long non-coding RNA and microRNA-675/let-7a mediates the protective effect of melatonin against early brain injury after subarachnoid hemorrhage via targeting TP53 and neural growth factor. Cell Death Dis [Internet]. 2018 [cited 2023 Jun 27];9. Available from: https://pubmed.ncbi.nlm.nih.gov/29367587/
76. Xu H, Stamova B, Ander BP, Waldau B, Jickling GC, Sharp FR, et al. mRNA Expression Profiles from Whole Blood Associated with Vasospasm in Patients with Subarachnoid Hemorrhage. Neurocrit Care. 2020;33:82–9.
77. Pulcrano-Nicolas A-S, Jacquens A, Proust C, Clarençon F, Perret C, Shotar E, et al. Whole blood levels of S1PR4 mRNA associated with cerebral vasospasm after aneurysmal subarachnoid hemorrhage. J Neurosurg. 2019;1–5.
78. Li H, Wang J, Li S, Cheng L, Tang W, Feng Y. Upregulation of microRNA-24 causes vasospasm following subarachnoid hemorrhage by suppressing the expression of endothelial nitric oxide synthase. Mol Med Rep. 2018;
79. Braun PR, Han S, Hing B, Nagahama Y, Gaul LN, Heinzman JT, et al. Genome-wide DNA methylation comparison between live human brain and peripheral tissues within individuals. Transl Psychiatry. 2019;9.

80. Ma B, Wilker EH, Willis-Owen SAG, Byun HM, Wong KCC, Motta V, et al. Predicting DNA methylation level across human tissues. Nucleic Acids Res. 2014;42:3515–28.